Journal of Building Engineering 15 (2018) 311–317

Contents lists available at ScienceDirect

Journal of Building Engineering

journal homepage: www.elsevier.com/locate/jobe

# Flexural behaviour of geopolymer concrete beams exposed to elevated temperatures

George Mathew[a], Benny Joseph[b,*]

[a] Division of Safety and Fire Engineering, School of Engineering, Cochin University of Science and Technology, Cochin 682022, Kerala State, India
[b] Department of Civil Engineering, VKCET, Thiruvananthapuram 691574, Kerala State, India

ARTICLE INFO

*Keywords:*
Geopolymer
Fly ash
Concrete beam
High temperature
Flexure
Crack width

ABSTRACT

Flexural behaviour of fly ash based geopolymer concrete beams exposed to elevated temperatures (200 °C, 400 °C, 600 °C and 800 °C) has been discussed in this paper. Beams of size 150 mm (W) × 200 mm (D) × 1100 mm (L) were cast with 0.52% reinforcing steel. Cover to the reinforcement has been varied (20 mm, 30 mm and 40 mm) and the geopolymer concrete used had a cube compressive strength of 57 MPa. The deformation characteristics, moment–curvature relationship and cracking behaviour were observed. It could be concluded that, the deformation characteristics of reinforced geopolymer concrete beams at ambient temperature is similar to that of the reinforced cement concrete beams and could be predicted using strain compatibility approach. However, when they are exposed to elevated temperatures, the strain compatibility approach underestimates the deformation behaviour of reinforced geopolymer concrete beams. Further, ductility of the geopolymer concrete beams reduces rapidly with the increase in exposure temperature. Approximate equation has been proposed to predict the service load crack width of geopolymer concrete beams after exposure to elevated temperatures.

## 1. Introduction

Consumption of concrete in the world is second to water [1]. Production of cement, the binder material in concrete releases almost equal quantity of $CO_2$ to the atmosphere [17]. As a result, different methods to minimize the use of cement in concrete, either partially or fully have been attempted by many researchers [23]. One of such methods is to use geopolymer (GP) concrete. Geopolymer completely replaces cement in concrete and can be considered as an environment friendly construction material than Ordinary Portland Cement (OPC) concrete. Geopolymer, the binding material in geopolymer concrete, is formed by alkali activation of amorphous alumino-silicate material under warm atmosphere. It has been reported that, the geopolymer concrete having compressive strength up to or even greater than 60 MPa could be easily produced [13,4].

Fly ash is one of the alumino-silicate materials for making geopolymer [23]. Fly ash is generated as a waste product at thermal power stations and its effective disposal is a major concern across the world due to the environmental and health hazard issues caused by it [16]. Use of fly ash as an alumino-silicate material for producing geopolymer binder is an effective method of utilizing a waste material.

Geopolymer concrete is considered to be a promising construction material in place of cement concrete due to its better performance like resistance against acidic and sulphate exposure [19,22,3]; better shrinkage and creep properties [13], etc. However, limited information is available on the flexural behaviour of geopolymer concrete.

Sumajouw et al. [25] conducted test on reinforced geopolymer concrete (RGC) beams of size 200 mm × 300 mm × 3000 mm. They reported that the deformation and cracking behaviour of reinforced geopolymer concrete beam is similar to that of reinforced cement concrete (RCC) beam.

Chang [8] conducted study on the shear characteristics of RGC beams and has observed that their shear characteristics are almost similar to that of RCC beams.

Sumajouw et al. [24] conducted uniaxial bending test on 175 mm × 175 mm × 1500 mm size RGC columns and have reported that the load caring capacity of RGC column correlate well with the value calculated based on the stability analysis as well as the values calculated based on the Australian standard and the ACI Building codes (for RCC). They have suggested that the RGC can be used in place of RCC for columns.

Structural members are likely to be exposed to high temperatures due to either functional or accidental cause like fire. High temperature exposure may affect the flexural strength, shear strength, cracking behaviour, ductility etc. of flexural members [12,20,5,21]. However, sufficient information is not available at present on the behaviour of geopolymer concrete beams after exposure to elevated temperatures.

* Corresponding author.
*E-mail address:* bennykollam@yahoo.co.in (B. Joseph).

https://doi.org/10.1016/j.jobe.2017.09.009
Received 23 December 2016; Received in revised form 29 August 2017; Accepted 16 September 2017
Available online 21 September 2017
2352-7102/ 

**Table 1**
Chemical composition of fly ash.

| Sl. no. | Parameter | Content (% by mass) |
|---|---|---|
| 1 | $SiO_2$ | 59.70 |
| 2 | $Al_2O_3$ | 28.36 |
| 3 | $Fe_2O_3 + Fe_2O_4$ | 4.57 |
| 4 | CaO | 2.10 |
| 5 | $Na_2O$ | 0.04 |
| 6 | MgO | 0.83 |
| 7 | $Mn_2O_3$ | 0.04 |
| 8 | $TiO_2$ | 1.82 |
| 9 | $SO_3$ | 0.40 |
| 10 | Loss of ignition | 1.06 |

Present paper reports the details of an investigation on the flexural behaviour of fly ash based geopolymer concrete beams after exposure to elevated temperatures.

## 2. Experimental program

In the present study, fly ash based GP concrete beams were cast and were exposed to elevated temperatures at a constant rate of temperature incr ease (5.5 °C/min). Once the set temperature is reached (200 °C, 400 °C, 600 °C and 800 °C), the specimens were cooled to ambient temperature by air cooling. The specimens were then tested at ambient temperature under two point loading and various flexural parameters were observed.

### 2.1. Materials

Low calcium fly ash (ASTM Class F) obtained from a thermal power station in India has been used for the present study. The chemical composition of fly ash, as determined by X-Ray Fluorescence (XRF) analysis is presented in Table 1 and the particle size distribution is shown in Fig. 1. The fly ash used for the present study had 55% glass phase, which could be observed from the XRD spectrum presented in Fig. 2. The fly ash used had a specific gravity of 1.9.

A mixture of NaOH and $Na_2SiO_3$ solution was used as alkali solution in the present investigation. NaOH pellets of 98% purity were used to make sodium hydroxide solution. $Na_2SiO_3$ had 34.64% $SiO_2$, 16.27% Na2O and 49.09% water. The specific gravity of alkali liquid solution varies slightly with change in molarity of NaOH solution and for the molarity10, the specific gravity was 1.54.

Crushed granite aggregate of nominal size 20 mm was used as coarse aggregate. Natural river sand was used as fine aggregate. The fineness modulus of fine aggregate was 2.38. The specific gravity of coarse and fine aggregate was 2.70 and 2.58 respectively. The coarse and fine aggregate had 0.19% and 0.86% water absorption respectively.

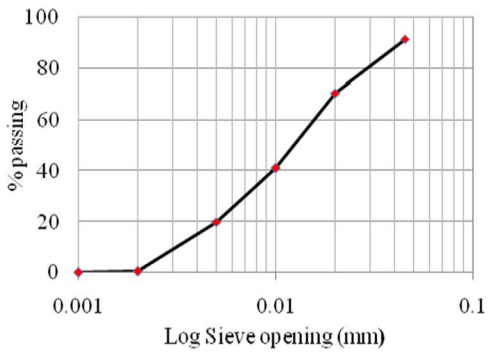


**Fig. 1.** Particle size distribution of fly ash.

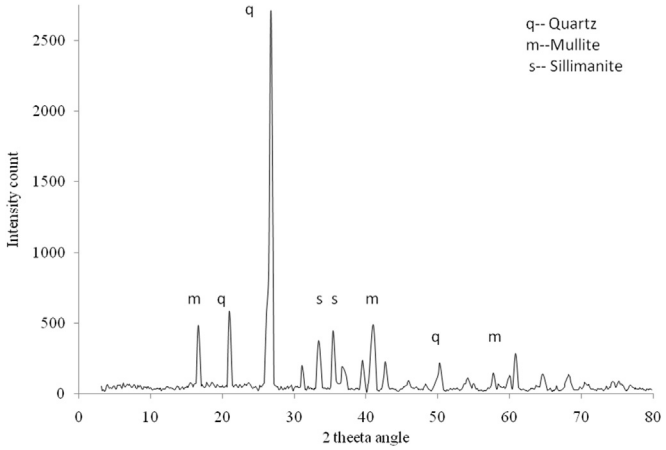


**Fig. 2.** XRD spectrum of fly ash.

### 2.2. Mix proportioning

Preliminary study has been conducted to arrive at the optimum proportion of the various constituents of GP concrete and its details are reported elsewhere [14]. Accordingly, the parameters that kept constant in the present investigation includes the aggregate content by volume (= 70%), the ratio of fine aggregate to total aggregate (= 0.35), the ratio of alkali to fly ashy by mass (= 0.55), the molarity of NaOH (= 10), the ratio of $Na_2SiO_3$ to NaOH (= 2.5), and the ratio of water to geopolymer solid (= 0.25). The quantity of materials required to produce 1 $m^3$ of GP concrete based on the above proportions is given in Table 2.

The prepared 10 M NaOH solution was first mixed with the calculated amount of $Na_2SiO_3$ liquid, stirred well and kept for 24 hours before use. Coarse and fine aggregates in saturated surface dry condition were thoroughly mixed with fly ash in a pan mixture. The alkali liquid and a Naphthalene based superplastisizer (2% by weight of fly ash) were mixed together and then added to the dry mix and the whole materials were mixed together for 5 minutes.

### 2.3. Casting and temperature curing

Reinforced geopolymer concrete beams of size 150 mm (W) × 200 mm (D) × 1100 mm (L) were cast in steel moulds. Deformed steel bars were used for reinforcement. Two number of 10 mm diameter bars were used as bottom reinforcement with two 8 mm bars as top hanger bars. The shear reinforcement in the form of closed stirrup was made of 6 mm diameter bars and was spaced at 80 mm center to center. Fig. 3 depicts the reinforcement details of the GP concrete beam cast. Three groups of beam were cast with a variation in the clear cover to bottom reinforcement in each group (20 mm, 30 mm and 40 mm). In each group, 5 beam specimens were cast. 150 mm size cubes were also cast along with beam specimen to determine the strength of GP concrete. After placing the steel reinforcement cage in position, fresh GP concrete was poured into the mould and vibrated using a needle vibrator. Both

**Table 2**
Quantity of material for 1 $m^3$ of GP concrete.

| Material | Quantity (kg/$m^3$) |
|---|---|
| Coarse aggregate | 1204.00 |
| Sand | 648.35 |
| Fly ash | 309.85 |
| NaOH solution (10 M) | 48.69 |
| Sodium silicate | 121.72 |
| Super plasticizer | 6.20 |
| Extra water | 3.80 |

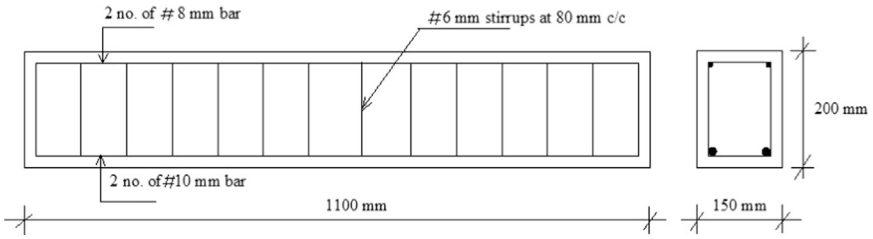


**Fig. 3.** Reiforcement detais of GP concrete beam.

beam and cube specimens were kept under laboratory condition for 60 min and then, after covering with thin steel plate, they were subjected to heat curing in an electric oven at 100 °C for a period of 24 h.

The curing temperature and curing period were arrived at based on a preliminary study [14]. After temperature curing, the specimens were kept at room temperature till they were tested.

### 2.4. Heating and testing of beam specimens

Geopolymer concrete beams and corresponding cube specimens were heated in an electric furnace to preset temperatures of 200 °C, 400 °C, 600 °C and 800 °C. The Specimens were heated at constant rate of temperature increase (5.5 °C/min). After attaining the target temperature, specimens were kept at the same temperature for one hour to ensure a uniform temperature throughout the specimen. The heated specimens were then taken out from the furnace and cooled down to ambient temperature by air cooling. Reinforcing steel bars of diameter 10 mm and 8 mm were also kept in the furnace along with concrete specimens for the determination of the residual strength of reinforcing steel at different temperature exposures. The mechanical properties of reinforcing steel after exposure to elevated temperatures are presented in Table 3.

The GP concrete beams were tested under two point load, applied at one third span. Fig. 4 shows the experimental setup for the specimens.

Demountable mechanical gauge (DEMEC) of 200 mm gauge length was used for measuring strain across the depth of the beam at the mid span of the specimen.

The beam was subjected to an incremental load of 3 kN. After every load increment, DEMEC gauge readings were taken. Observations like deflection, load at first crack, crack width, crack propagation etc. were also noted at every load increment.

## 3. Result analysis

Table 4 shows the load at first crack and ultimate load on GP concrete beam tested after exposure to different temperatures.

From Table 4 it could be observed that, the load at first crack at ambient temperature reduces marginally with increase in clear cover to the reinforcement. However, for temperature above 200 °C, GP concrete beam with a clear cover of 30 mm shows slightly higher load capacity to crack compared to beams with 20 mm and 40 mm cover.

The ultimate load on beams after exposure to temperatures above 200 °C is also slightly higher for beam with 30 mm cover compared to that of beams with 20 mm and 40 mm cover. However, considering the possible variation in the test results, it could be concluded that, the variation of cover to reinforcement up to 40 mm has no significant influence on first crack load and on the ultimate load of GP beam after exposure to elevated temperatures.

**Table 3**
Mechanical properties of reinforcing steel after exposure to elevated temperatures.

| Exposure temperature (°C) | Yield strength of steel (MPa) | Modulus of elasticity of steel (MPa) |
|---|---|---|
| Ambient (28) | 460 | 205,240 |
| 200 | 460 | 205,090 |
| 400 | 440 | 202,620 |
| 600 | 400 | 188,490 |
| 800 | 360 | 172,250 |


**Fig. 4.** Experimetal set up for loading of GP concrete beam.

It could be noted from Table 4 that, even though the cube compressive strength of GP concrete is not reduced between 600 °C and 800 °C (because of further polymerization of initially unreacted materials), the load caring capacity of beams reduces rapidly beyond 600 °C. This could be primarily due to the rapid strength reduction of reinforcing steel in the beam at these temperatures.

Fig. 5 shows typical load deflection graph of GP concrete beams after exposure to elevated temperatures. As expected, for a given load, the deflection is more for a GP concrete beam exposed to higher temperature. Larger deformation with temperature increase is due to the development of more number of micro cracks as well as due to the reduced strength of materials (concrete and steel) at elevated temperatures. It may be noted from Fig. 5 that, the rate of increase of deflection of beam slightly reduces when the temperature is increased from 600 °C to 800 °C as against the rate of increase of deflection of beam exposed to a temperature up to 600 °C. This behaviour is more predominant after the initiation of crack and is primarily due to the slight strength gain of GP concrete beyond 600 °C.

Fig. 6 shows typical moment curvature (m-φ) relationship of GP concrete beam after exposure to elevated temperatures. It could be seen from Fig. 6 that, for lower temperature exposures, the m-φ relationship shows a bilinear curve, which is similar to RCC beams [15]. Further, a definite yield stage could be observed for GP concrete beams when they are exposed to a temperature up to 400 °C. However, beyond 400 °C, the cracking stage could be identified and the m-φ curve becomes multi-linear. Further, a clear yield stage of the beams is not visible in m-φ relationship for temperature exposure beyond 400 °C. The curvature of the beam also increases beyond 400 °C. This is due to the development of more number of internal cracks as well as due to the low residual strength of materials beyond 400 °C.

Fig. 7 compares the experimental m-φ relationship of beam with the theoretical values for two extreme temperature ranges considered in the present study as a typical case. For specimens exposed to a temperature within the extreme temperatures presented, the m-φ relationship also

**Table 4**
Load at fist crack and ultimate load on geopolymer concrete beam.

| Temperature | Cubecompressive strength of GP concrete (MPa) | Load at fist crack (kN) | | | Ultimate load (kN) | | |
|---|---|---|---|---|---|---|---|
| | | 20 mm cover | 30 mm cover | 40 mm cover | 20 mm cover | 30 mm cover | 40 mm cover |
| Ambient | 57.30 | 45 | 43 | 40 | 101 | 99 | 98 |
| 200 °C | 42.52 | 42 | 42 | 36 | 94 | 95 | 92 |
| 400 °C | 37.33 | 36 | 39 | 33 | 92 | 92 | 78 |
| 600 °C | 30.82 | 33 | 36 | 33 | 85 | 90 | 75 |
| 800 °C | 32.88 | 30 | 33 | 30 | 68 | 75 | 66 |

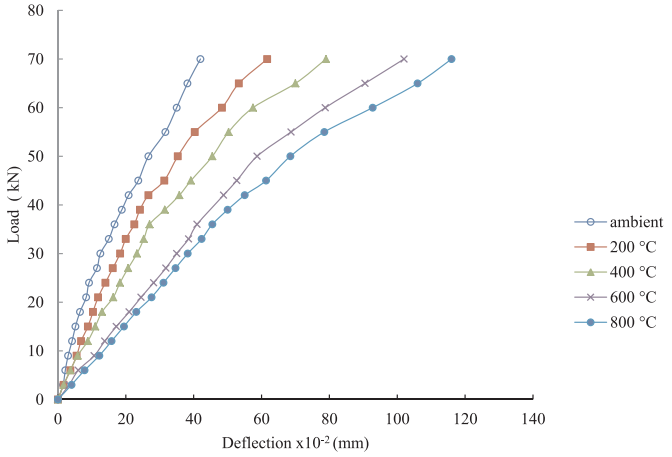


**Fig. 5.** Typical load deflection curve of geopolymer concrete beam after exposure to elevated temperatures.

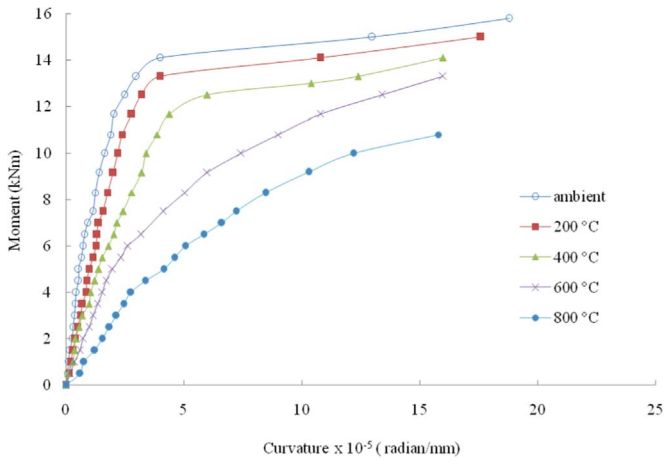


**Fig. 6.** Typical moment curvature curve of GP concrete beam after exposure to elevated temperatures.

lies between these two extreme curves. The theoretical m-φ curves were obtained based on strain compatibility criteria [18] and by considering the strength and modulus of elasticity of the materials corresponding to the respective exposure temperatures.

From Fig. 7, it could be observed that, the experimental m- φ relationship has been predicted correctly using strain compatibility approach at ambient temperature. However, as the exposure temperature increases, the theoretical values underestimate the curvature up to the yield moment. It may be noted that, while theoretical curve shows a bilinear behaviour, experimental curve (800 °C temperature exposure) shows a multi-linear variation. However, towards the ultimate moment, the theoretical value approaches the experimental value.

Fig. 8 compares the curvature of beams at cracking stage and yielding of reinforcement after exposure to different temperatures.

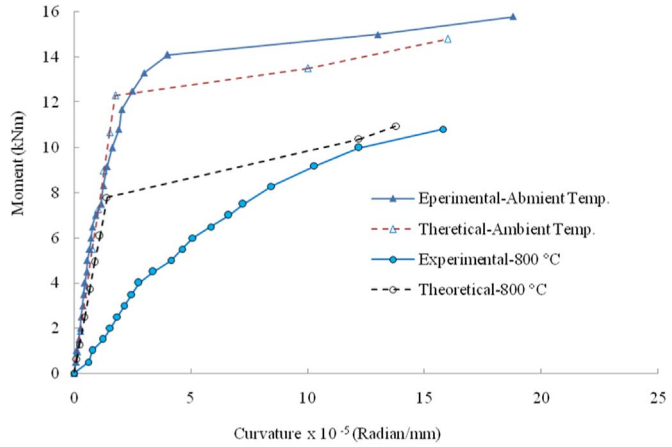


**Fig. 7.** Typical experimental and theoretical moment curvature relationship of GP concrete beam after exposure to ambient and 800 °C temperatures.

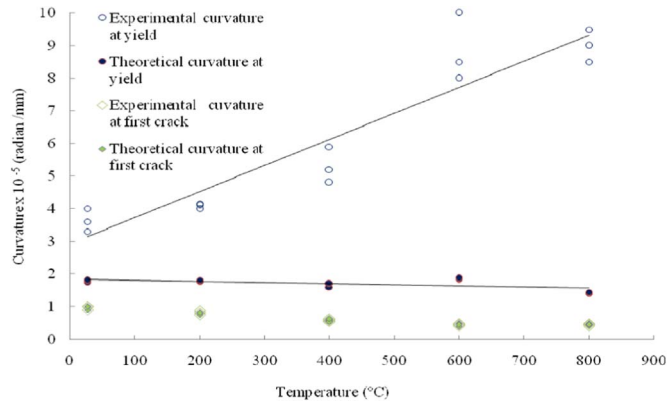


**Fig. 8.** Variation of experimental and theoretical curvature at first crack of beam and at yielding of reinforcement with different temperature of exposure.

From this figure, it is clear that, the curvature of GP concrete beams varies linearly with temperature for loads between the cracking stage of concrete and yielding of reinforcement. However, this variation is not predicted in the theoretical calculation of curvature for beams loaded between cracking stage and the stage corresponding to the yielding of reinforcement.

Ultimate moment of resistance of GP concrete has been calculated theoretically in a way similar to the calculation for RCC beams and by considering the strength and modulus of elasticity of the materials corresponding to the respective exposure temperatures. It may be noted that there is only marginal difference between the predicted experimental values (within 12%). Hence it could be concluded that, the m-φ relationship of geopolymer concrete beam at ambient temperature behaves similar to RCC beams and it could be predicted well by adopting the strain compatibility criteria. However, as the exposure temperature increases, the theoretical method (strain compatibility method) very much underestimates the curvature between the values corresponding

**Table 5**
Ductility ratio of GP concrete beam after exposure to different temperatures.

| Exposure Temperature (°C) | Mu (kN m) | My (kN m) | Mu/My | Φu (radian/mm) | Φy (radian/mm) | φu/φy |
|---|---|---|---|---|---|---|
| Ambient (28) | 15.8 | 14.1 | 1.12 | 0.000188 | 0.000040 | 4.7 |
| 200 | 15 | 13.3 | 1.13 | 0.000176 | 0.000040 | 4.4 |
| 400 | 14.1 | 12.2 | 1.16 | 0.000165 | 0.000048 | 3.4 |
| 600 | 13.3 | 11.2 | 1.19 | 0.00016 | 0.000080 | 2.0 |
| 800 | 10.83 | 9.6 | 1.13 | 0.000158 | 0.000095 | 1.7 |

to first cracking of the beam and yielding of the reinforcement.

Table 5 shows the ductility ratio of GP concrete beam (typical) after exposure to elevated temperatures. The ultimate curvature has been considered as the curvature corresponding to 95% of the ultimate load. It could be observed from Table 5 and Fig. 6 that, both ultimate moment (Mu) and yield moment (My) reduces more or less at a constant ratio with temperature. However, the ductility of GP concrete beam reduces as the exposure temperature increases. This is because of the fact that, while the curvature at yielding of steel ($\varphi_y$) increases with temperature, the curvature at ultimate stage ($\varphi_u$) reduces.

Different codes of practices propose different permissible maximum crack width based on the exposure conditions. These maximum permissible crack widths range from 0.1 mm to 0.3 mm in BS [7] and BIS (IS 456 2000) code of practices and ranges from 0.1 mm (0.04 in) to 0.4 mm (0.16 in) in the case of ACI code (ACI 318 [2]).

Once the beams are exposed to elevated temperatures, existing cracks, if any, may widen under service load, leading to unacceptable serviceability conditions. So a beam after exposure to elevated temperature may have to have either reduced service load or to have additional protection, primarily corrosion protection to the reinforcing steel. Hence it is important to understand the extent of the crack development at service load stage after beams are exposed to elevated temperatures. Fig. 9 shows typical crack pattern of GP concrete beam. It could be observed from Fig. 9 that, the crack pattern is similar to that of RCC beam.

To the best of the authors‟ knowledge, there is no equation available to predict the crack width of GP concrete beam after exposure to elevated temperatures. Hence the suitability of available equations for RCC beams has been checked for the crack width prediction of geopolymer concrete beams. The equations proposed by different investigators and code of practices [10,11,6,9] have been considered in the present study. As these equations are proposed primarily for crack width calculation at ambient temperature, appropriate residual strength parameters of GP concrete and steel at elevated temperatures were used in these equations for predicting the crack width at elevated temperatures.

Figs. 10 and 11 show typical graph comparing the experimental results with the theoretically calculated crack width at different exposure conditions and for different values of cover to the reinforcement.

It could be observed from these figures that, while some predictions underestimate the crack width, some overestimates. However, the rates of development of crack width with temperatures calculated based on the equations considered is more or less the same as that of the

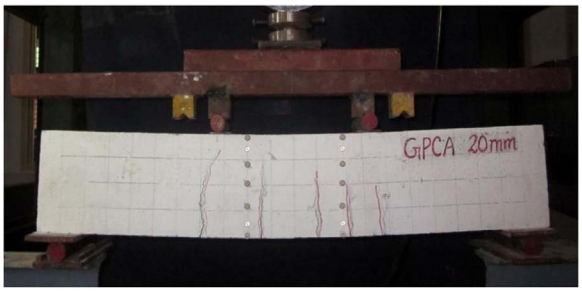


**Fig. 9.** Crack pattern in GP concrete beam.

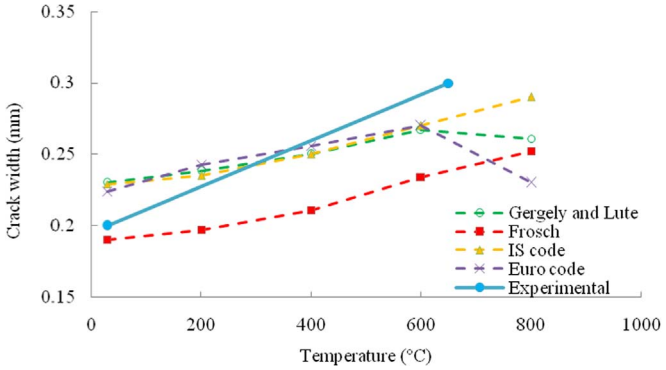


**Fig. 10.** Comparison of theoretical and experimental crack width at different temperature exposure (30 mm cover).

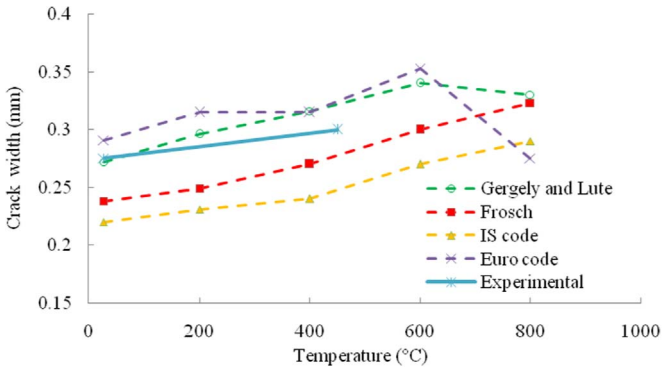


**Fig. 11.** Comparison of theoretical and experimental crack width at different temperature exposure (40 mm cover).

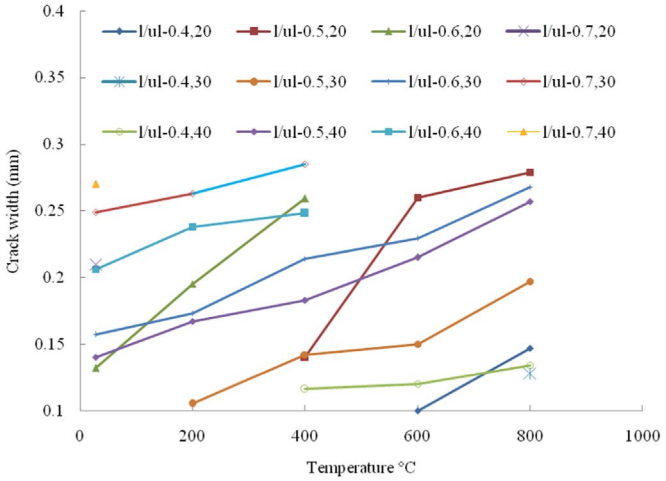


**Fig. 12.** Variation of crack width with temperature for different load ratios and cover to the reinforcement.

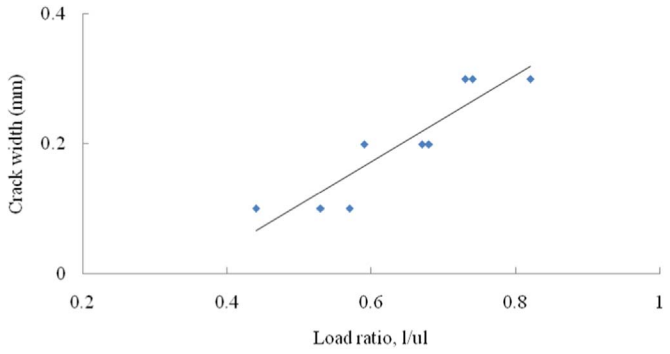


**Fig. 13.** Variation of crack width with load/ultimate load curve.

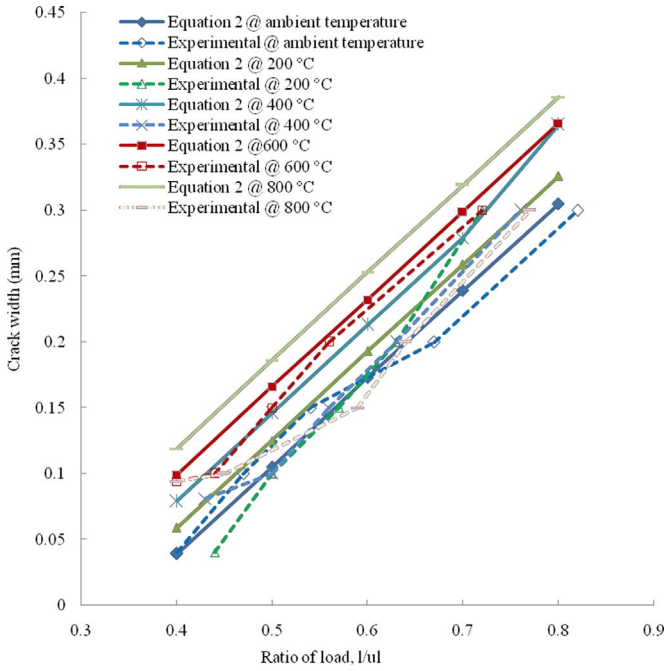


**Fig. 14.** Comparison of crack width based on Eq. (2) and experimental values.

experimental curve.

Fig. 12 shows the variation of the crack width (from 0.1 mm to 0.3 mm) with respect to the exposure temperature of GP concrete beams. The variation of crack width with temperature has been plotted for beams with different cover (20 mm, 30 mm and 40 mm) and for load ratios (ratio of applied load to the ultimate load -l/ul) ranging from 0.4 to 0.7. The logic behind considering the load ratio between 0.4 and 0.7 is to consider the load ratios corresponding to the service load conditions (by assuming the service load as 2/3rd of the ultimate load -l/ul = 0.67).

From Fig. 12, it could be observed that the development of crack width is almost in a linear pattern with temperature rise for all beams (with cover 20 mm to 40 mm) and under the load ratios considered (l/ul from 0.4 to 0.8). Hence, if the average slope of the curves is known, it is possible to assess the increased width of crack of GP concrete beam due to temperature exposure. In the present investigation, the average slope of the curve could be assessed as 1 in 1000.

Fig. 13 shows the scatter diagram of the crack width verses the load ratio of GP concrete beams tested at ambient temperature. From this scatter diagram, it could be seen that, a linear equation could be proposed to predict the crack width of GP beam at ambient temperature.

Accordingly, following approximate equation could be proposed for the determination of crack width of GP concrete beam subjected to service loads (load ratio between 0.4 and 0.8) at ambient temperature.

$$C_{wa} = (6667/10000)(l/ul) - (2274/10000) \text{ with } 0.4 < (l/ul) < 0.8 \quad (1)$$

where, $C_{wa}$ is the crack width at ambient temperature in mm and the equation is valid for a crack width between 0.1 mm and 0.3 mm.

Hence, the approximate values of the crack width of GP concrete at service loads and after exposure to an elevated temperature of T °C could be determined by the following equation.

$$C_{wt} = C_{wa} + (T/10000) \text{ with } 28 < T \leq 800 \quad (2)$$

where, $C_{wt}$ is the crack width in mm at a temperature exposure of T °C.

So using Eqs. (1) and (2), the service load on a GP concrete beam could be assessed (l/ul) after exposed to temperatures for a predicted maximum crack width ($C_{wt}$) and temperature exposure ( T). Fig. 14 shows the comparison of experimental values and the values based on Eq. (2). From the Fig. 13 it is clear that, Eq. (2) could be used for predicting crack width approximately after exposure to different temperatures.

## 4. Conclusions

Based on the study carried out on geopolymer concrete beams, following conclusions could be made Even though the cube compressive strength of geopolymer concrete is not reduced between 600 °C and 800 °C (because of polymerization of initially unreacted materials), the load caring capacity of geopolymer concrete beams reduces rapidly beyond 600 °C.

The primary factor contributing to the loss of load carrying capacity of geopolymer concrete beams exposed to temperatures above 600 °C is the strength reduction of the reinforcing steel.

The load corresponding to the development of first crack in a geopolymer concrete beams reduces with increase in exposure temperature and is dependent on the depth of concrete cover to the reinforcement. In the present study, at 800 °C temperature exposure, while beam with 20 mm cover cracked at 66% of the load corresponding to the cracking load at ambient temperature, the beam with 40 mm cover cracked only at 75% of the said load.

The moment–curvature relationship of geopolymer concrete beams at ambient temperature is similar to that of RCC beams and this could be predicted using strain compatibility approach.

Once geopolymer concrete beam is exposed to elevated temperatures, the strain compatibility approach underestimates its curvature between load at first cracking and load corresponding to the yielding of reinforcement.

With the increase in temperature, the ductility of the geopolymer concrete beams reduces rapidly.

As the exposure temperature increases, the geopolymer concrete beam experiences an increased value of yield curvature with a reduced ultimate curvature. For the present study, the geopolymer concrete beam lost its ductility by 64% after exposure to a temperature of 800 °C.

Approximate equation has been proposed to predict the service load crack width of geopolymer concrete beams after exposure to elevated temperatures. This equation could be used to limit the service load on geopolymer concrete beams for a pre defined crack width (from 0.1 mm to 0.3 mm) after the beam is exposed to an elevated temperature (up to 800 °C).

## Acknowledgements

This project was sponsored by Kerala State Council for Science, Technology and Environment (No. 55/2012/KSCSTE dated 23-01-2012.).

## References

[1] W.H. Plenge, Introducing vision 2030: our industry's 30-year map to the future, ACI Concr. Int. 23 (3) (2001) 25–34.
[2] ACI 318-95 and Commentary ACI 318R-08, Building Code Requirements for

Structural Concrete, American Concrete Institute, Detroit, 1995.
[3] T. Bakharev, Durability of geopolymer materials in sodium and magnesium sulfate solution, Cem. Concr. Res. 35 (6) (2005) 1233–1246.
[4] S.A. Bernal, R. Mejía de Gutiérrez, A.L. Pedraza, J.L. Provis, E.D. Rodriguez, S. Delvasto, Effect of binder content on the performance of alkali-activated slag concrete, Cem. Concr. Res. 41 (1) (2011) 1–8.
[5] D.N. Bilow, M.E. Kamara, Fire and concrete structures, in: Proceedings of the Structures Congress, Crossing Borders, Canada, April 24–26, 2008.
[6] BIS 456, Code of Practice for Plain and Reinforced Concrete, Bureau of Indian Standards, Newdelhi, 2000.
[7] BS 8110-2, Structural Use of Concrete, British Standard, London, 1985.
[8] E.H. Chang, Shear and Bond Behaviour of Reinforced Fly Ash-Based Geopolymer Concrete Beams, Thesis presented for the Degree of Doctor of Philosophy of Curtin University of Technology, Australia, 2009.
[9] Eurocode 2, Design of Concrete Structures – Part 1-1, General Rules and Rules for Buildings, European Committee for Standardization, Brussels, 1992.
[10] R.J. Frosch, Another look at cracking and crack control in reinforced concrete, ACI Struct. J. 96 (3) (1999) 437–442.
[11] P. Gergely, L.A. Lutz, Maximum Crack Width in RC Flexural Members, Causes, Mechanism and Control of Cracking in Concrete, SP-20, American Concrete Institute, 1968, pp. 87–117.
[12] L. Hana, Q. Tan, T. Song, Fire performance of steel reinforced concrete (SRC) structures, Proceedia Eng. 62 (2013) 46–55.
[13] D. Hardjito, S.E. Wallah, D.M.J. Sumajouw, B.V. Rangan, On the development of fly ash-based geopolymer concrete, ACI Mater. J. 101 (6) (2011) 467–472.
[14] B. Joseph, G. Mathew, Influence of aggregate content on the behaviour of fly ash based geopolymer concrete, Sci. Iran. 19 (5) (2012) 1188–1194.
[15] H.G. Kwak, S.P. Kim, Nonlinear analysis of RC beams based on moment–curvature relation, Comput. Struct. 80 (7) (2002) 615–628.
[16] B. Lokeshappa, A.K. Dikshid, Disposal and management of flyash, IPCBEE 3 (2011) 11–14.
[17] P.K. Mehta, Greening the concrete industry for sustainable development, ACI Concr. Int. 24 (7) (2002) 23–28.
[18] R. Park, T. Paulay, Reinforced Concrete Structures, John Wiley & Sons, USA, 1975.
[19] K.K. Patil, E.N. Allouche, Examination of chloride-induced corrosion in reinforced geopolymer concretes, J. Mater. Civ. Eng. 25 (10) (2013) 1465–1476.
[20] X. Shi, T. Tan, K. Tan, Z. Guo, Influence of concrete cover on fire resistance of reinforced concrete flexural member, J. Struct. Eng. 130 (8) (2004) 1225–1232.
[21] G. Shier, Flexural Behaviour of Fibre Reinforced Polymer Strengthened Reinforced Concrete beams at Elevated Temperatures, Thesis submitted to the Graduate Program in the Department of Civil Engineering in conformity with the requirements for the degree of Master of Applied Science, Queen's University, 2013.
[22] X.J. Song, M. Marosszekya, M. Brungsb, R. Munna, Durability of fly ash based Geopolymer concrete against sulphuric acid attack, in: Proceedings of 10DBMC International Conference on Durability of Building Materials and Components, LYON, France, 2005.
[23] D.M.J. Sumajouw, D. Hardjito, S.E. Wallah, B.V. Rangan, Geopolymer concrete for a sustainable future, Australas. Inst. Min. Metall. 3 (2011) 237–240.
[24] D.M.J. Sumajouw, D. Hardjito, S.E. Wallah, B. Rangan, Fly ash-based geopolymer concrete: study of slender reinforced columns, J. Mater. Sci. 42 (9) (2007) 3124–3130.
[25] M.D.J. Sumajouw, B.V. Rangan, Low-Calcium Fly Ash-based Geopolymer Concrete: Reinforced Beams and Columns. Research Report GC 3, Faculty of Engineering, Curtin University of Technology, Australia, 2006.